A Field Gradient Transformation of Large Array Magnetoencephalographic Data for Cortical Source Imaging

Moran, J.E. [1], Tepley, N.[1,2]

[1]*Department of Neurology, Henry Ford Hospital, Detroit, MI 48202, USA;*

[2]*Department of Physics, Oakland University, Rochester, MI 48309, USA*

Introduction

Development of mathematical techniques for MEG based imaging of neuronal activity has been spurred by increased availability of large array MEG systems. The accuracy of these techniques is affected by many factors, such as the forward model of magnetic fields from neuronal current sources that is employed. Noise in the MEG data is another significant factor affecting source imaging accuracy, especially if multiple cortical sources are simultaneously active. Multiple source techniques have been developed which attenuate the effect of noise by using the entire spatio-temporal MEG data set to identify sources [1, 2, 3]. However, a MEG imaging technique that utilizes a single time slice of data is more appropriate for estimating cortical source activity within a very short time interval.

Many MEG imaging techniques model the cortex as a dense three-dimensional lattice of single current dipoles. With the cortex represented as an array of thousands of single current dipoles, the magnetic field data, **b**, is a vector combination of signal, $\mathbf{b_s}$, and noise, **n**.

$$\mathbf{b} = \mathbf{b_s} + \mathbf{n} = \mathbf{G}(\mathbf{q_s} + \mathbf{q_n}) = \mathbf{Gq}. \quad (1)$$

G is a matrix containing the gain vectors for each cortical dipole source. $\mathbf{q_s}$ is a (non-unique) vector containing the cortical source amplitudes corresponding to the noise free signal. $\mathbf{q_n}$ is the error in the source amplitudes introduced by the noise. Unfortunately, MEG imaging techniques often introduce large noise source amplitudes, $\mathbf{q_n}$, even if the data contains only small or moderate amplitude noise. The noise sensitivity can be attenuated by introducing additional constraints on the solution of Equation 1 for the cortical source structure. We have devised a field gradient transformation technique to significantly attenuate noise in the data and introduce constraints on the source structure solution. After the large array of data is transformed, nearly all the signal power is concentrated in just a few of the field gradient data channels. However, the noise remains uniformly distributed among the full set of gradient channels. Thus, the influence of noise, $\mathbf{q_n}$, can be greatly reduced by applying this gradient transformation to Equation 1 and retaining only the high signal-to-noise gradient data channels and the corresponding field gradient gain matrix channels. However, as will be investigated and described, this transformation and channel truncation procedure introduces additional constraints on the source solution. In addition, reducing the number of independent data channels affects the ability to discriminate between cortical sources in the source structure. These source imaging and noise attenuation properties must be considered when applying this transformation to Equation 1. In this report, the field gradient transformation is applied to a simple, single current dipole model of large array neuromagnetometer data applied to a rectangular array of single current dipole sources with the same orientation.

Methods

The cortical source continuum was modeled as a 40 x 40 array of single current dipoles uniformly spaced on a 4 cm x 4 cm rectangular surface in an X,Y plane, centered 5 cm along the Z axis from the origin of a spherical volume conductor. The orientation of each current dipole was in the X direction. A MEG detector array was simulated with 91 first order gradiometers. The gradiometer baseline was 4 cm and 1.5 cm center to center detector spacing with the primary detector coils on a 10 cm spherical surface. The technique can readily be applied to different detector arrays. The detector array was centered over the cortical source grid, Fig. 1. For this detector and volume conductor geometry, the forward solution for the MEG amplitudes corresponding to each source in the array was performed. The current dipole amplitudes of the sources were adjusted such that the magnetic field amplitudes in the gain matrix **G** were equal power.

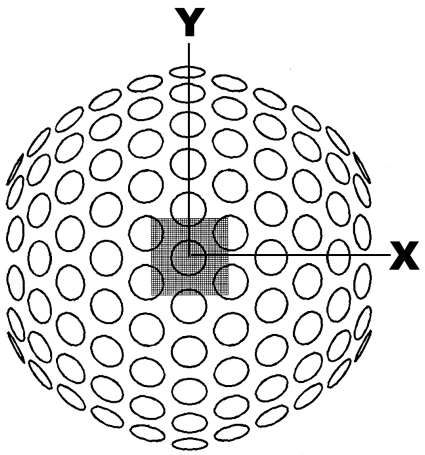

Fig. 1 91 channel MEG array and source grid.

In Equation 1, the simulated MEG data, **b**, corresponded to a single current dipole located at the center of the source grid oriented in the X direction with random noise added. A field gradient transformation matrix, **R**, was constructed and applied to both sides of Equation 1 from the left.

$$\mathbf{b_R} = \mathbf{R}\,\mathbf{b} = \mathbf{R}\,(\mathbf{b_s} + \mathbf{n}) = \mathbf{RG}(\mathbf{q_s} + \mathbf{q_n}) = \mathbf{G_R q}. \quad (2)$$

Each column vector of the field gradient transformation matrix, **R**, is constructed using an algorithm applied recursively to the magnetic field data, **b**. First, for a MEG array with N detector channels, the first column vector in **R** would have

N identical component amplitudes equal to $N^{1/2}$. Next, these N detector channels are split into two subsets, N^+ and N^-. Corresponding to this split the second column vector of **R** is constructed with the N^+ channels having amplitudes equal to $(N^-/N^+N)^{1/2}$ and the N^- channels having amplitudes of $(N^+/N^-N)^{1/2}$. Using this same splitting algorithm, the third column vector of **R** is constructed by splitting the N^+ subset. However, in this third column vector all channel amplitudes corresponding to the N^- subset are zero. The fourth column vector of **R** is constructed by splitting the N^- subset. The last column vectors of **R** corresponding to the splitting of subsets containing only two channels. These columns of **R** have only two non-zero channels amplitudes, plus and minus $2^{1/2}$. This field gradient transformation produces a unitary matrix. Thus it has the following properties:

$$\mathbf{R^T R = I} \text{ and } \mathbf{R R^T = I} \qquad (3)$$

Further, each column vector of **R** corresponds physically to a magnetic field gradient between specific N^+ and N^- subsets of channels. In Equation 2, the first few field gradient amplitudes of the magnetic field vector, $\mathbf{b_R}$, are significantly greater than all the others and have the highest signal-to-noise ratio. Therefore, the transformation matrix, **R**, can be truncated to $\mathbf{R_T}$. The lost spatial information from the data is primarily noise. However, for the magnetic fields in the transformed gain matrix, $\mathbf{G_R}$, additional field gradient amplitudes are usually required to avoid a significant reduction in magnetic field power. Thus, truncation of **R** to $\mathbf{R_T}$ introduces a bias in the source solution that favors those sources whose magnetic fields are well represented by the truncated set of field gradients, $\mathbf{R_T}$. In summary, the truncated field gradient transformation increases the signal-to-noise of the data and constrains the source solution to those sources with magnetic fields well resolved within the field gradient basis, $\mathbf{R_T}$. The vectors in **R** are similar to a wavelet decomposition of time series data [4].

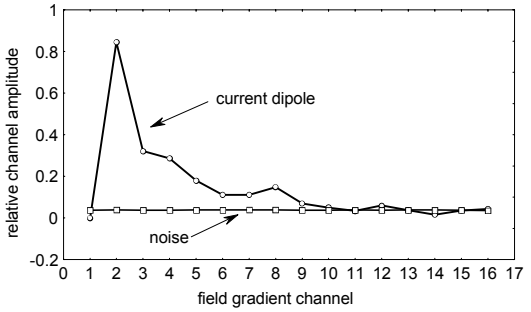

Fig. 2 Field gradient noise and signal amplitudes

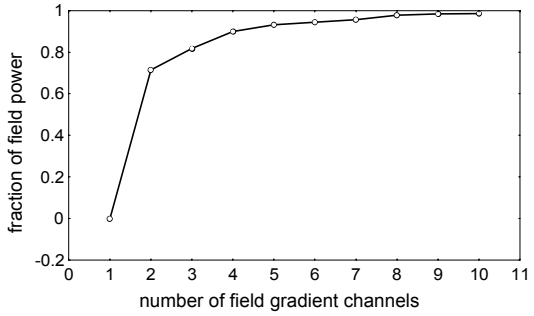

Fig. 3 Cumulative field gradient power versus number of channels

Results

An optimum field gradient transform for use in Equation 2, can only be constructed with noise free data. Applying this optimum transform to the magnetic field data with or without noise would concentrate the noise free signal into the least number of gradient channels. As an example, an optimum gradient transformation matrix, **R** was constructed using noise free magnetic field data of a single current dipole. In Equation 2, $\mathbf{Rb = R\,b_s + Rn}$. Therefore, this transformation was applied separately to the noise free signal and compared to the average transformation of 1000 sets of random noise, adjusted to correspond to a noise level of 20 percent signal power. This comparison data is plotted in Fig. 2. The noise is uniformly distributed among all field gradient channels. However, the magnetic field power of the single current dipole is concentrated into just a few field gradient channels. In Fig. 3, over 90 percent of the single dipole magnetic field power is contained in four field gradient channels. For data containing 20 percent random noise, the fraction of field gradient channel power is less than five percent in each of the first eight gradient channels, (Fig. 4). Thus, retaining only the first few high signal-to-noise channels primarily affects only the noise on the left side of Equation 2. However, on the right side of this equation, application of the truncated transform matrix, **R**, to the gain matrix, **G**, alters the relative power of the individual magnetic field vectors in $\mathbf{G_R}$. Magnetic fields most similar to the data are relatively unaffected by the transformation. In addition to this amplitude weighting effect, fewer independent components are available in $\mathbf{G_R}$ to spatially resolve source structure. These two factors can be separated, such that,

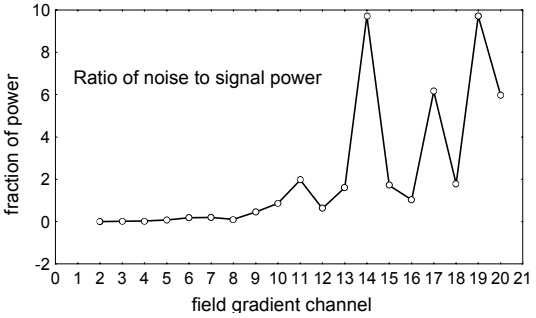

Fig. 4 Fraction of noise in each field gradient channel

$$\mathbf{G_R = W_P G_U}$$

$\mathbf{W_P}$ is a diagonal weight matrix with amplitudes proportional to the transformed power.

$\mathbf{G_U}$ is a uniform power transformed gain matrix.

Fortunately, the weighting effect bias's the solution in favor of sources whose gain matrix is most similar to the magnetic field data and can compensates for the limited source resolution based on $\mathbf{G_U}$. These features are demonstrated in Fig. 5. **G**, $\mathbf{G_R}$ and $\mathbf{G_U}$ were calculated for sources along the X axis of the source grid. $\mathbf{G_R}$ and $\mathbf{G_U}$ incorporate only four field gradient amplitudes in each field gradient gain vector column. The cross product of these

gain matrices with the corresponding normal magnetic field data, $\mathbf{b_0}$ (or field gradient data, $\mathbf{b_{0R}}$), of the X = 0 source are plotted in Fig. 5. In Fig. 5, the normal field data correlation, $\mathbf{G^T b_0}$ (normal data), is a maximum at X = 0 and changes rapidly with position, (good spatial resolution). The graph of $\mathbf{G_U{}^T b_{0R}}$ (unit grad), exhibits a very slow amplitude change with position, (poor spatial resolution). Only four field gradient amplitudes quantify the magnetic field patterns and these cross product amplitudes. However, the weight factor is included in $\mathbf{G_R}$, such that, the spatial variation of $\mathbf{b_0 G_R}$ is similar to the normal data correlation, (good spatial resolution).

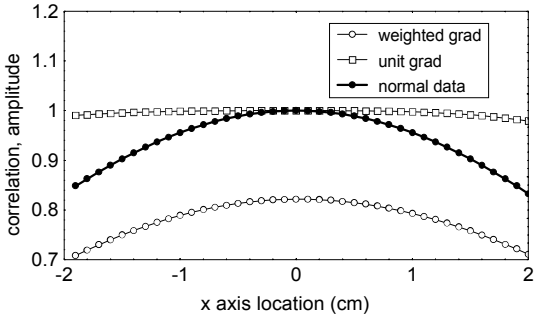

Fig. 5 Spatial resolution of field gradient data versus normal data

Unfortunately, in real imaging applications the field gradient matrix, **R**, must be generated using magnetic field data that include noise. Thus, the composition of the gradient vectors is **R** is influenced by the relative amplitude of the noise versus the noise free data. Therefore, the ability of the truncated gradient transformation to filter noise from the data is significantly degraded as the fraction of noise increases. In Fig. 6, the vertical axis is the fraction of noise power remaining in the transformed data and the horizontal axis is the fraction of noise in the normal 91 channel magnetic field data. Notice that the noise filtering performance degrades exponentially rather than linearly as would occur for the optimum field gradient transformation. In addition, as additional field gradient components are added this filter performance line approaches a straight line with a slope of 1(no noise filtered).

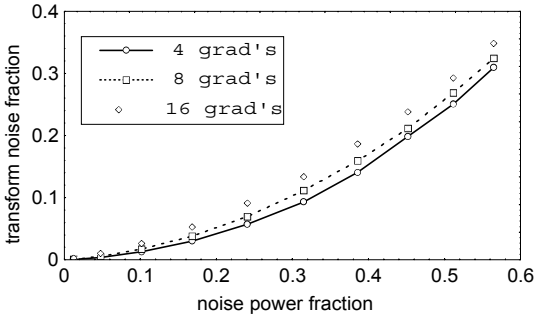

Fig. 6 Fraction of noise in field gradient data versus original data

Finally, the ability to use the transformed data, Equation 2, to solve for the inverse of the single dipole model is examined. In Fig. 7, the single current dipole location error is plotted versus the relative fraction of random noise power included in the data. Unlike multiple dipole models, the single dipole model is relatively insensitive to noise with accuracy increased by adding channels. Therefore, it is important that application of the field gradient transformation does not significantly degrade the performance of this single source technique. These data demonstrate, with as few as 4 field gradient components, source location accuracy is affected only slightly compared to the accuracy based on the full array 91 magnetic field data set.

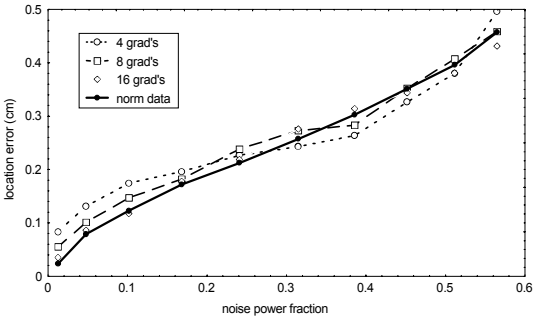

Fig. 7 Source location error versus fraction of noise in the data

Discussion

These results demonstrate the potential use of the field gradient transformation in MEG source imaging. These results demonstrate that using a small number of field gradient amplitudes does not necessarily result in a loss of spatial resolution or reduced accuracy of source solutions of the transformed data, Equation 2, relative to source solutions of the normal data, Equation 1. However, the use of this transformation in multi-source imaging techniques requires further investigation. In particular, regularization techniques must be incorporated to avoid excessive sensitivity to noise. The ability of the field gradient transformation to substitute for regularization techniques must be determined. Also, the interaction between the weighting factors introduced by this transformation and other constraints on the solution of Equation 2 must be studied

References

[1] Hämäläinen M., Hari R., Ilmoniemi R.J., Knuutila J. and Lounasmaa O.V. Magnetoencephalography – theory, instrumentation, and applications to noninvasive studies of the working human brain Rev. Mod. Phys., 1993, 65: No. 2 413-495

[2] Lütkenhöner B. Dipole and Multidipole source analysis of Magnetic Fields: Possibilities and Limitations. In: C. Baumgartner, L. Deecke, G. Stroink, S.J. Williamson (Eds.), Biomagnetism: Fundamental Research and Clinical Applications. Elsevier , IOS Press, Amsterdam, The Netherlands, 1995, 376 – 380.

[3] Mosher J.C., Lewis P.S., Leahy R.M. Multiple dipole modeling and localization from spatio-temporal MEG data. IEE Trans. Biomed. Eng., 1992, 39: 541-557

[4] Press W.H., Teukolsky S.A., Vetterling W.T., Flannery B.P. Wavelet Transforms in: Numerical Recipes in C, 2nd ed., 1996(b), 591-606

Acknowledgement

Research supported by NIH/NINDS grant R01 NS30914